Hyperelastic Tuning of One-Dimensional Phononic Band Gaps Using Directional Stress

Andriejus Demčenko, Michael Mazilu, Rab Wilson, Arno W. F. Volker, and Jonathan M. Cooper

***Abstract*— In this paper, we show that acoustoelasticity in hyperelastic materials can be understood using the framework of nonlinear wave mixing, which, when coupled with an induced static stress, leads to a change in the phase velocity of the propagating wave with no change in frequency. By performing Floquet wave eigenvalue analysis, we also show that band gaps for periodic composites, acting as 1-D phononic crystals, can be tuned using this static stress. In the presence of second-order elastic nonlinearities, the phase velocity of propagating waves in the phononic structure changes, leading to observable shifts in the band gaps. Finally, we present numerical examples as evidence that the band gaps are tuned by both the direction of the stress and its magnitude.**

***Index Terms*— Floquet waves, hyperelasticity, nonlinear ultrasound, phononic crystals.**

I. Introduction

MULTILAYERED periodic composites can be represented as 1-D phononic crystals [1], [2], comprising heterogeneous arrays of materials with different elastic properties. Such composites are increasingly being used in the automotive, marine, and aerospace industries as load bearing structures. For example, metal-polymer layered structures are now used in the fuselage of aircraft [3]. Similarly in the semiconductor industry, multilayered microstructures with different lattice spacings or with different thermal expansion coefficients that will induce differential stresses either during manufacture or in service. The lifetime and performance of such structures will depend upon the applied and/or the residual static stresses, induced either during their manufacture [4] and/or during their operation [5]. The detection of unwanted static stress states is key in determining the risk of failure in many of these safety-critical structures [6] as this may lead to the propagation of defects [7], which will ultimately affect their structural or functional performance.

Manuscript received March 22, 2018; accepted March 26, 2018. Date of publication April 17, 2018; date of current version June 1, 2018. This work was supported in part by the Engineering and Physical Sciences Research Council Fellowship under Grant EP/K027611/1 and in part by the European Research Council advanced investigator award under Grant 340117. *(Corresponding author: Andriejus Demčenko.)*

A. Demčenko, R. Wilson, and J. M. Cooper are with the Division of Biomedical Engineering, School of Engineering, The University of Glasgow, Glasgow G12 8LT, U.K. (e-mail: andriejus.demcenko@glasgow.ac.uk).

M. Mazilu is with the SUPA, School of Physics and Astronomy, University of St. Andrews, St. Andrews KY16 9SS, U.K.

A. W. F. Volker is with Acoustics and Sonar, TNO, 2597 AK Den Haag, The Netherlands.

Digital Object Identifier 10.1109/TUFFC.2018.2821440

Composite structures can be represented as 1-D phononic crystals, which can contain measurable band gaps [8] for ultrasonic waves. The spectral features of the ultrasound after interacting with the phononic structure will represent characteristics of its inherent periodic structure. Thus, when composite structures experience an applied or residual static stress, the ultrasonic wave propagation velocities will change within the different layers, as the characteristic of the band gap changes.

In this paper, starting from the nonlinear equations of motion [9], we deduce the dispersion relationships in such 1-D phononic structures in the presence of the static stress, which can be described as a zero-frequency wave [10]. These equations allow us to interpret the phenomena of acoustoelasticity in terms of a nonlinear wave mixing process [9] between a propagating wave and a zero-frequency wave. During this mixing, the output frequency does not shift, but the phase velocity of the propagating wave changes. The effect is enhanced by the presence of periodicity within the composite (which acts as a 1-D phononic crystal). As a consequence of the interplay between the phononic crystal and the ultrasonic nonlinear response to the static stress, the effect becomes observable, and indeed, provides a method of characterizing changes in the composite.

Using this principle, we now develop a new model to enable us to analyze how the composite, represented as a band gap in a 1-D phononic crystal, depends upon the applied static stress. Our analysis is underpinned using a nonlinear wave mixing [9] together with a recently revised acoustoelasticity theory in biaxially stressed, hyperelastic platelike structures [11] and Floquet (Floquet–Bloch) wave theory for an infinite periodic medium [12].

Using this understanding of band gaps in composites potentially introduces an important new method for structural health monitoring. The fact that the band gaps can be controlled actively by the application of a static stress may also, in the future, lead to development of stress sensitive metamaterials [13]. In order to implement this concept, we used a recursive stiffness matrix method [14] to calculate the Floquet wavenumbers and reflection coefficients from a periodic semi-space. Despite the acoustoelastic effect being small [15], numerical analysis shows that the band gaps were very sensitive both to the static stress direction and to its magnitude—thus showing the potential of this method to detect defects in periodic composites. The model was also validated using

data from the previously reported works [11], [16] and these results are presented in Appendix A.

II. Method

The nonlinear equation of motion for an ideal isotropic solid is given in [9]

$$\rho\frac{\partial^2 v_i}{\partial t^2}-\mu\frac{\partial^2 v_i}{\partial x_j\partial x_j}-(\lambda+\mu)\frac{\partial^2 v_j}{\partial x_i\partial x_j}=\frac{\partial\sigma_{ij}}{\partial x_j} \tag{1}$$

where ρ is the density of the undeformed medium, $\mathbf{v}$ is the displacement vector in the solid, $x_1 = x$, $x_2 = y$, $x_3 = z$, and t are the space and time coordinates, and λ and μ are the Lamé constants. We use here the summation over repeated indices convention. The left-hand side corresponds to the linear wave equation and the right-hand side to the divergence of the nonlinear stress tensor given as

$$\begin{aligned}\sigma_{ij}(\mathbf{v}) &= (\mu+A/4)\left(\frac{\partial v_s}{\partial x_i}\frac{\partial v_s}{\partial x_j}+\frac{\partial v_i}{\partial x_s}\frac{\partial v_j}{\partial x_s}+\frac{\partial v_i}{\partial x_s}\frac{\partial v_s}{\partial x_j}\right)\\ &+\frac{A}{4}\frac{\partial v_s}{\partial x_i}\frac{\partial v_j}{\partial x_s}+C\frac{\partial v_s}{\partial x_s}\frac{\partial v_r}{\partial x_r}\delta_{ij}\\ &+\frac{B+\lambda}{2}\left(\frac{\partial v_s}{\partial x_r}\frac{\partial v_s}{\partial x_r}\delta_{ij}+2\frac{\partial v_i}{\partial x_j}\frac{\partial v_s}{\partial x_s}\right)\\ &+\frac{B}{2}\left(\frac{\partial v_s}{\partial x_r}\frac{\partial v_r}{\partial x_s}\delta_{ij}+2\frac{\partial v_j}{\partial x_i}\frac{\partial v_s}{\partial x_s}\right)\end{aligned} \tag{2}$$

where A, B, and C are the third-order elastic constants in Landau and Lifshitz notation [17].

In order to model the nonlinear interaction between the static strain and an ultrasonic wave, we consider

$$\mathbf{v}=\mathbf{e}\cdot\mathbf{r}+\mathbf{u}e^{-\mathrm{i}(\omega t-\mathbf{k}\cdot\mathbf{r})} \tag{3}$$

where $\mathbf{e}$ is a diagonal static strain tensor with the terms (e_{11}, e_{22}, and e_{33}) on the diagonal. Using (1) and (2), we define a modified dispersion relationship linking the static strain to the phase velocity for a wave propagating in the x_1-direction (detailed calculations presented in these results are presented in Appendix B)

$$\begin{aligned}\rho c_L^2 &= 2Ae_{11}+(2B+\lambda)(3e_{11}+e_{22}+e_{33})\\ &+2C(e_{11}+e_{22}+e_{33})+6e_{11}\mu+\rho c_{0L}^2\end{aligned} \tag{4}$$

$$\begin{aligned}\rho c_S^2 &= (A/2+2\mu)(e_{11}+e_S)\\ &+(B+\lambda)(e_{11}+e_{22}+e_{33})+\rho c_{0S}^2\end{aligned} \tag{5}$$

where the subscript S corresponding to the shear wave is either 22 or 33, and c_{0L} and c_{0S} are the longitudinal and shear wave velocities, respectively, in the unstressed medium. We show that nonlinear wave mixing and the induction of static stress lead to an effective change in the phase velocity of the propagating wave with a zero-frequency shift [10]. We note that propagation along different directions or nondiagonal stress tensors can also be deduced in a similar manner; however, the dispersion relations, (4) and (5), will contain more terms and the stressed media will show anisotropic properties.

To analyze the elastic wave propagation in these hyperelastic 1-D phononic crystals, we implement a recursive stiffness matrix method. The Floquet wave equation is given as [14]

$$A_3\cos(3k_{zF}H)+A_2\cos(2k_{zF}H)+A_1\cos(k_{zF}H)+A_0=0 \tag{6}$$

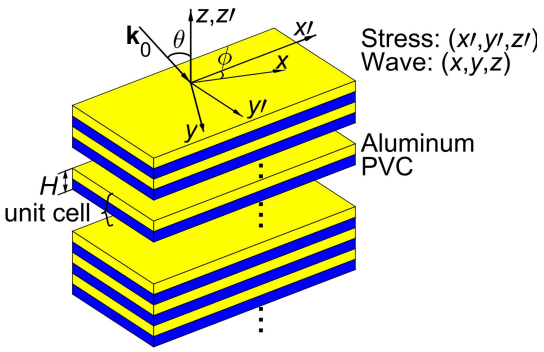

Fig. 1. Two-layered unit cell of the periodic medium and coordinate system for the static stress and wave propagation directions. $\mathbf{k}_0$ is the incident wave and θ is the wave incidence angle from the fluid. The stress is specified in the primed coordinate system and guided waves propagate along x-direction at any arbitrary angle ϕ from x'-direction. The analysis is conducted in the unprimed coordinate system (x, y, z), hence the primed coordinate system is rotated through the angle ϕ. The coordinate system is selected so that the xz plane coincides with the wave incident plane, hence $k_y = 0$.

where k_{zF} is the vertical Floquet wavenumber and H is the unit cell thickness (Fig. 1). The following are the Floquet wave coefficients, A_i, (these have been modified and updated from those originally reported [18]) in terms of the unit cell stiffness matrix

$$A_3=\left|\mathbf{K_c^{21}}\right| \tag{7}$$

$$A_2=1/2\left(\left|\mathbf{M}+\mathbf{K_c^{21}}\right|+\left|\mathbf{M}-\mathbf{K_c^{21}}\right|\right)-\left|\mathbf{M}\right| \tag{8}$$

$$A_1=1/2\left(\left|\mathbf{M}+\mathbf{K_c^{21}}\right|-\left|\mathbf{M}+\mathbf{K_c^{12}}\right|+\left|\mathbf{K_c^{21}}-\mathbf{K_c^{12}}\right|\right)-\mathbf{2}\left|\mathbf{K_c^{21}}\right| \tag{9}$$

$$A_0=1/4\left(\left|\mathbf{M}+\mathbf{K_c^{12}}-\mathbf{K_c^{21}}\right|+\left|\mathbf{M}-\mathbf{K_c^{12}}+\mathbf{K_c^{21}}\right|\right)-A_2 \tag{10}$$

where $\mathbf{M}=\mathbf{K_c^{22}}-\mathbf{K_c^{11}}$, $|\mathbf{M}|$ is the determinant of matrix $\mathbf{M}$ and $\mathbf{K_c}$ is the whole stiffness matrix of the unit periodic cell [14].

The amplitude reflection coefficient from a submersed semispace in terms of the Floquet wave equation parameters [19] can thus be written in the following form:

$$R_{\mathrm{as}}=\frac{S_F^{33}-\cos\theta/(i\omega\rho_F c_F)}{S_F^{33}+\cos\theta/(i\omega\rho_F c_F)} \tag{11}$$

where θ is the wave incidence angle (Fig. 1), $\omega = 2\pi f$, f is the wave frequency, ρ_F is the volumetric mass density, and c_F is the wave speed. S_F^{33} is the (3, 3) element in the 3×3 surface compliance matrix for a homogeneous or layered anisotropic semispace.

As an example of a 1-D phononic crystal (see Fig. 1), we now show results for a two-layered unit cell of the metal polymer periodic medium containing an aluminum and a polyvinylchloride (PVC) layer of 0.1 mm thickness. The following second-order elastic material properties were used in the eigenvalue analysis of the Floquet waves in the 1-D hyperelastic phononic structure: $\lambda_1 = 54.307$ GPa, $\mu_1 = 27.174$ GPa, and $\rho_1 = 2704$ kg/m^3; whilst $\lambda_2 = 3.8745$ GPa, $\mu_2 = 1.6335$ GPa, and $\rho_2 = 1350$ kg/m^3 for the aluminum and PVC layers, respectively [9], [11]. The corresponding

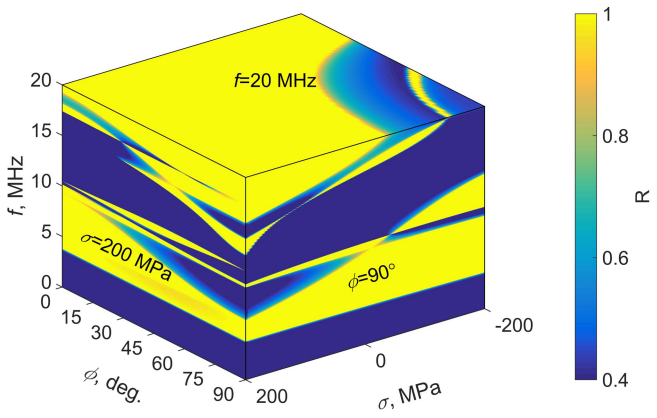

Fig. 2. Band gaps in the periodic semispace loaded by fluid when the wave incidence angle $\theta = 35°$. $R = 1$ and $R < 1$ zones correspond to stopbands and passbands, respectively.

third-order elastic constants are in Murnaghans notation [20]: $l_1 = -281.5$ GPa, $m_1 = -339$ GPa, and $n_1 = -416$ GPa and $l_2 = -33.43$ GPa, $m_2 = -20.88$ GPa, and $n_2 = -15.86$ GPa. The relationships between the third-order elastic constants in Landau and Lifshitz and Murnaghan's notations are given in Appendix C. The above semispace fluid properties are $c_F = 1480$ m/s and $\rho_F = 1000$ kg/m^3.

III. Results

In our analysis three scenarios were investigated, namely: 1) using an applied static stress σ_{22}, which is constant and equal to 200 MPa (tensile case), but where we vary both the angle ϕ (see Fig. 1) in the range $0° - 90°$ with $1°$ increments and the incident wave frequency f in the range 0–20.0 MHz with 1 kHz increments (this scenario corresponds to $\phi - f$ plane); 2) using an angle ϕ which is constant and equal to 90°, but where we vary both the stress σ_{22} in the range -200–200 MPa with 4.35 MPa increments and the incident wave frequency varies in the range 0–20.0 MHz, with 1 kHz increments (this scenario corresponds to $\sigma - f$ plane); and 3) the scenario where the frequency of the incidence wave is kept constant and equal to 20 MHz, and where we vary both the angle ϕ in the range 0°–90° and the stress σ_{22} in the range $-200 - +200$ MPa (the last scenario corresponds to $\sigma - \phi$ plane). In all three scenarios, the wave incidence angle was $\theta = 35°$ (to provide a representative illustration of the influence of the acoustoelastic effect on band gaps in the periodic semispace).

Fig. 2 shows the subsequent 3-D plot of the energy reflection coefficient from the fluid loaded stressed periodic semispace. We used a static stress limit of ± 200 MPa, which can be either be an applied or residual stress within the structure [21].

For band gaps which correspond to zones where $R = 1$, passbands are formed where $R < 1$. The results also show that the band gaps have a strong dependence (band gap becomes 2.5 times narrower due to the stress) on the static stress and the wave propagation direction ϕ (Fig. 1) in the periodic semispace ($\phi - f$ plane). The band gaps depend significantly on the stress value when $\phi = 90°$, see plane $\sigma - f$ in Fig. 2.

When $\sigma = 0$ MPa, the energy reflection coefficient corresponds to the unstressed semispace case. When the incidence wave frequency f is equal to 20.0 MHz (plane $\sigma - \phi$), the results also show that a band gap is formed in a wide range of the parameters σ and ϕ. The results are presented in more detail for the second scenario, which demonstrates the corresponding response for compression and tensile stress case in $\phi - f$ plane.

Furthermore, we represent the ultrasonic wave response of the periodic structure in terms of Floquet wavenumbers, where the unit cell thickness product $\Re(k_{zF} \times H)$ and energy reflection coefficients R from a periodic semispace loaded by a fluid when the angle $\phi = 90°, 45°, 0°$, see Fig. 1. Two separate cases are considered in the analysis with respect to the angle ϕ, namely, when the shear horizontal wave motion is not coupled to the sagittal wave motion [Fig. 3(a)–(c) and (g)–(i)], and second, when coupling occurs between the shear horizontal and sagittal wave motions [22] [Fig. 3(d)–(f)]. In the reference case, where $\sigma_{22} = 0$ MPa, and $m_{o,i}$ and $m_{i,j}$ denote the out-of-plane shear wave and in-plane shear and longitudinal wave modes, respectively. Modes in both compressive and tensile cases are denoted as $n_{o,i}$ and $n_{i,j}$. For the reference case, the 1-D phononic crystal contains three well-defined zones [see Fig. 3(a)] comprising an effective homogeneous medium from 0 to 3.7 MHz, [see Fig. 3(b), mode m_{i1}]; the first band gap in the frequency range 3.7–9.1 MHz, and finally, the main passband in the frequency range 10.0–17.1 MHz.

When the static stress direction is coincident with the wave propagation direction ($\phi = 90°$), Fig. 3(a)–(c), significant changes occur in the band gap zones of the phononic crystal, despite the shear wave motion being decoupled from the sagittal wave motion. In this case, however, the first band gap is almost unaffected in the compression stress. However, in the tensile case, this band gap reduces from 3.7–9.1 MHz to 3.8–5.9 MHz, becoming 2.5 times narrower. This is due to a change in the mode dispersion of the structure as shown in Fig. 3(b) of the stressed mode n_{i2} with respect to the same reference mode m_{i2}. The tensile static stress [Fig. 3(c)] also shifts down the second band gap which occurs in the frequency range 12.4–13.9 MHz, see the modes m_{i3}, m_{i4} and n_{i3}, n_{i4}. The compression stress [Fig. 3(a)] causes a significant band-gap shift in the frequency range 10–13.3 MHz, this is shown in Fig. 3(b) where the reference mode m_{i3} is shifted up, but the dispersion remains unchanged, whereas m_{i2} mode does not shift significantly but its dispersion is changed. The out-of plane modes $m_{o,i}$ are relatively insensitive to the applied stress in comparison with $m_{i,j}$ modes.

In the case of the $m_{i,j}$ modes, the results show that the smallest difference in ultrasonic response from the stressed periodic structures is observed when the wave propagation and stress directions are orthogonal ($\phi = 0°$) [see Fig. 3(g)–(i)]. In this case, the $m_{o,i}$ modes are sensitive to the applied stress and these modes are consequently significantly shifted (see the modes n_{o2} and n_{o3}).

Finally, when the angle $\phi = 0°$ or $\phi = 90°$, the modes present in the structure are pure. However, when the angle ϕ deviates from these values, the modes no longer remain pure and the shear horizontal wave motion couples into the

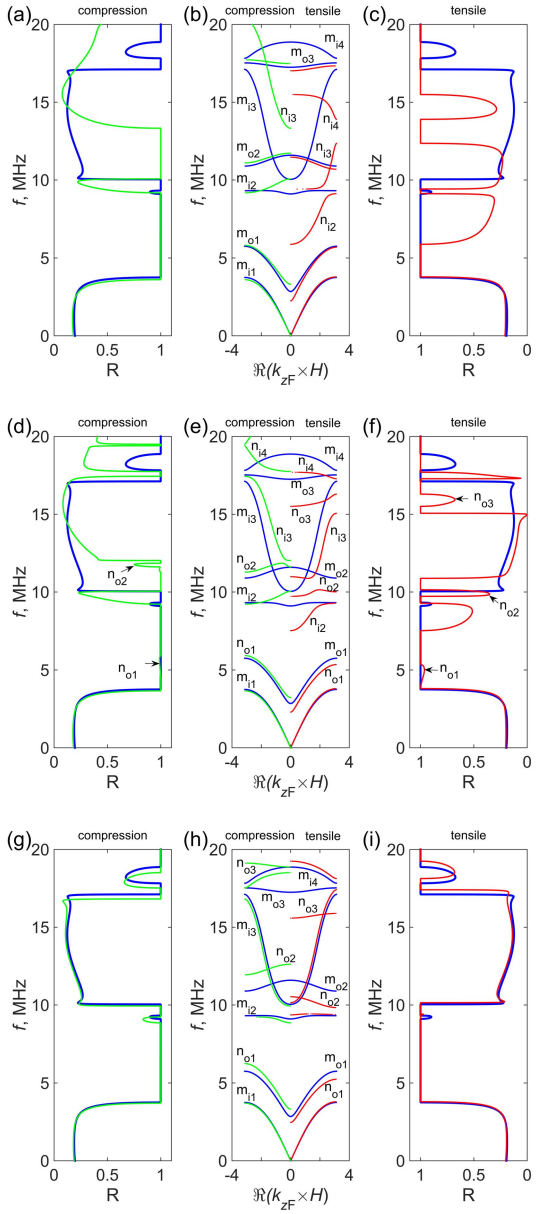

Fig. 3. Ultrasonic response from a periodic semispace loaded by fluid when the incident beam angle $\theta = 35°$ and angle ϕ is (a)–(c) $\phi = 90°$, (d)–(f) $\phi = 45°$, and (g)–(i) $\phi = 0°$. The energy reflection coefficients for the compression case [(a), (d), and (g)] and tensile stress case [(c), (f), and (i)] are shown. The corresponding Floquet wavenumber and unit cell thickness product $\Re(k_{zF} \times H)$ is depicted in (b), (e), and (h). Blue curves: the reference case when $\sigma_{22} = 0$ MPa. Green curves: the response when $\sigma_{22} = -200$ MPa. Red curves: the response $\sigma_{22} = 200$ MPa.

sagittal wave motion. For example, this coupling is shown for the case when $\phi = 45°$ in the reflection coefficient, for the frequency range 3.8–5.3 MHz [Fig. 3(f), mode n_{o1}] in the tensile stress case (where weaker coupling is observed in the compression stress case). The modes n_{o2} and n_{o3} have a higher coupling to the sagittal wave motion. In the compression stress case [Fig. 3(d)], the first band gap is less affected than in the tensile stress case. The results show that in the tensile stress case, the first band gap is formed in the frequency range 5.3–7.5 MHz, and it is 2.5 narrower compared with the band gap when $\sigma_{22} = 0$ [see Fig. 3(f)]. The narrowing

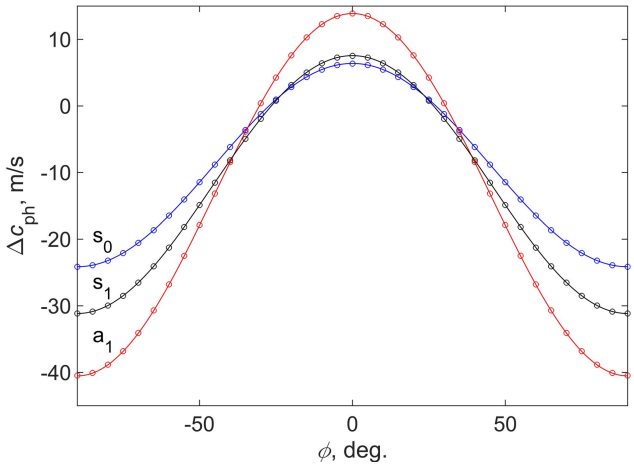

Fig. 4. Lamb wave phase velocity dependence on the angle ϕ in aluminum plate of thickness 6.35 mm when $\sigma_{11} = 57.5$ MPa, where circles indicate the reported data from [11]. Calculations are performed at the following frequencies: 0.25 (s_0 mode), 0.4 (a_1 mode), and 0.6 MHz (s_1 mode).

is caused by a change in the m_{i2} reference mode dispersion, see n_{i2}. The main passband is also narrower as is seen in the frequency ranges 12.0–17.4 MHz and 10.9–15.0 MHz for the compression and tensile stress cases, respectively. These latter changes occur due to m_{i3} mode shifting up in the case of compression stress, and shifting down in the case of tensile stress, see mode n_{i3}.

IV. Conclusion

In conclusion, we show that static stress together with second-order material nonlinearities have a significant influence on the band gaps in 1-D phononic crystals. This acoustoelastic effect can be understood as the nonlinear wave mixing between a zero-frequency wave and a propagating wave. Our results extend recently reported work [13], where analysis was conducted using small amplitude motions in a normal direction, while we now consider finite amplitude elastic waves having oblique angle propagation.

We show that the band gaps are highly tunable with respect to the direction and the magnitude of static stress. We also show that the effect is enhanced both by the resonances in the 1-D phononic crystals and by the coupling between the shear horizontal and sagittal wave. In the future, our study has the potential to enable a number applications in industries using periodic composites structures, including the integrity of large-scale composite structures used in the aerospace industry or of stresses caused by thermal mismatches in microstructures created within the semiconductor industry.

Appendix A
Validation of the Implementation of the Stiffness Matrix Method for Guided and Floquet Waves in Layered Structures

Fig. 4 shows the Lamb wave phase velocity dependence for three modes, two of which are symmetric, s_0 and s_1, and one that is antisymmetric a_1, with respect to the angle

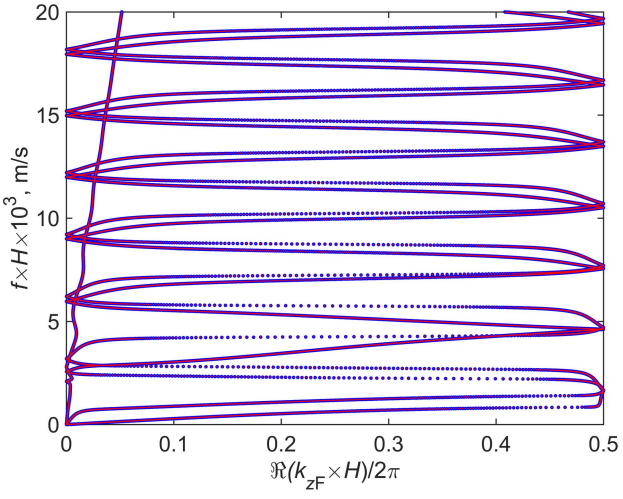

Fig. 5. Relation between $\Re(k_{zF} \times H)$ and $f \times H$. Red color: data from [16]. The viscoelastic unit cell comprises aluminum and epoxy of equal thickness. The incidence angle is 80° corresponding to longitudinal wave in nylon.

ϕ in a single-layered aluminum plate when applied stress $\sigma_{11} = 57.5$ MPa. The material properties are listed in [11]. Our results, carried out as replicates, show an excellent agreement with the reported results in [11], see Fig. 10.

Fig. 5 also shows Floquet wavenumbers for the two-layered viscoelastic unit cell comprising aluminum and epoxy layers of equal thickness. The incidence angle of longitudinal wave in nylon is 80°. The material properties are listed in [16]. Our results show an excellent agreement with the reported results in [16], see Fig. 2(b).

Appendix B
Static Strain Dispersion Relations

Using the ultrasonic wave and static strain superposition defined by (3), we can determine separately the linear and nonlinear effects in equation of motion (1). To simplify the notations, we consider the longitudinal and shear waves separately. In the case of longitudinal waves propagating in the x_1-direction, we have the linear part equal to

$$\rho \frac{\partial^2 v_i}{\partial t^2} - \mu \frac{\partial^2 v_i}{\partial x_j \partial x_j} - (\lambda + \mu) \frac{\partial^2 v_j}{\partial x_i \partial x_j} = u_i e^{-\mathrm{i}(\omega t - \mathbf{k}\cdot\mathbf{r})} k^2 \left(\lambda + 2\mu - \rho c_{0L}^2\right) \quad (12)$$

where the polarization amplitude $\mathbf{u}$ is parallel to the wave vector $\mathbf{k}$. Similarly, we can determine the nonlinear stress tensor for the superposition (3)

$$\frac{\partial \sigma_{ij}}{\partial x_j} = -u_i e^{-\mathrm{i}(\omega t - \mathbf{k}\cdot\mathbf{r})} k^2 (2C(e_{11} + e_{22} + e_{33}) 2A e_{11} + (2B + \lambda)(3e_{11} + e_{22} + e_{33}) + 6e_{11}\mu). \quad (13)$$

Equating (12) and (13) allows us to introduce a new static strain dependent wave velocity, c_{0L}, as defined by (4). The wave part of the superposition is then a solution of the linear wave equation taking this modified velocity into account.

In the same way, we proceed to evaluate the effect of the static strain on shear waves. In this case, the linear part of the wave equation evaluates to

$$\rho \frac{\partial^2 v_i}{\partial t^2} - \mu \frac{\partial^2 v_i}{\partial x_j \partial x_j} - (\lambda + \mu) \frac{\partial^2 v_j}{\partial x_i \partial x_j} = u_i e^{-\mathrm{i}(\omega t - \mathbf{k}\cdot\mathbf{r})} k^2 \left(\mu - \rho c_{0S}^2\right) \quad (14)$$

where the polarization amplitude $\mathbf{u}$ is perpendicular to the wave vector $\mathbf{k}$. The nonlinear stress tensor for the superposition (3) in this case is equal to

$$\frac{\partial \sigma_{ij}}{\partial x_j} = -u_i e^{-\mathrm{i}(\omega t - \mathbf{k}\cdot\mathbf{r})} k^2 (A/2 + 2\mu)(e_{11} + e_S) + (B + \lambda)(e_{11} + e_{22} + e_{33}) \quad (15)$$

where the subscript S corresponding to the shear wave direction with indices equal to either 22 or 33. Similar to the longitudinal case, equating (14) and (15) allows us to introduce a new static strain dependent wave velocity c_{0S} as defined by (5). The wave part of the superposition is then a solution of the linear wave equation taking this modified velocity into account.

Appendix C
Relationship Between Third-Order Elastic Constants for Isotropic Solids

The relationships between the third-order elastic constants in Landau and Lifshitz (A, B, and C) and Murnaghan's notations are given as

$$l = B + C, \quad m = A/2 + B, \quad n = A \quad (16)$$

where l, m, and n are the third-order elastic constants in Murnaghan's notations.

Acknowledgment

The authors would like to thank Dr. J. Michaels from Georgia Tech and Dr. E. L. Tan from Nanyang Technological University for providing data used in Figs. 4 and 5, and also thank Dr. M. Tassieri for his helpful discussions. All data created during this research are openly available from the University of Glasgow at http://dx.doi.org/10.5525/gla.researchdata.600.

References

[1] J. H. Page *et al.*, "Phononic crystals," *Phys. Status Solidi B*, vol. 241, no. 15, pp. 3454–3462, Dec. 2004.
[2] Y. Pennec, J. O. Vasseur, B. Djafari-Rouhani, L. Dobrzyński, and P. Deymier, "Two-dimensional phononic crystals: Examples and applications," *Surf. Sci. Rep.*, vol. 65, no. 8, pp. 229–291, 2010.
[3] L. B. Vogelesang and A. Vlot, "Development of fibre metal laminates for advanced aerospace structures," *J. Mater. Process. Technol.*, vol. 103, no. 1, pp. 1–5, 2000.
[4] S. U. Khan, R. C. Alderliesten, and R. Benedictus, "Delamination growth in fibre metal laminates under variable amplitude loading," *Compos. Sci. Technol.*, vol. 69, nos. 15–16, pp. 2604–2615, 2009.
[5] P. Peddiraju, J. Noh, J. Whitcomb, and D. Lagoudas, "Prediction of cryogen leak rate through damaged composite laminates," *J. Compos. Mater.*, vol. 41, no. 1, pp. 41–71, 2007.
[6] T. Zhang, Q. Zhu, W. L. Huang, Z. Xie, and X. Xin, "Stress field and failure probability analysis for the single cell of planar solid oxide fuel cells," *J. Power Sour.*, vol. 182, no. 2, pp. 540–545, 2008.

[7] A. Evans and J. Hutchinson, "The thermomechanical integrity of thin films and multilayers," *Acta Metallurgica Et Mater.*, vol. 43, no. 7, pp. 2507–2530, 1995.
[8] M. S. Kushwaha, P. Halevi, L. Dobrzynski, and B. Djafari-Rouhani, "Acoustic band structure of periodic elastic composites," *Phys. Rev. Lett.*, vol. 71, pp. 2022–2025, Sep. 1993.
[9] V. Korneev and A. Demčenko, "Possible second-order nonlinear interactions of plane waves in an elastic solid," *J. Acoust. Soc. Amer.*, vol. 135, no. 2, pp. 591–598, 2014.
[10] J. Rivière *et al.*, "Frequency, pressure, and strain dependence of nonlinear elasticity in berea sandstone," *Geophys. Res. Lett.*, vol. 43, no. 7, pp. 3226–3236, 2016.
[11] N. Gandhi, J. E. Michaels, and S. Lee, "Acoustoelastic Lamb wave propagation in biaxially stressed plates," *J. Acoust. Soc. Amer.*, vol. 132, no. 3, pp. 1284–1293, 2012.
[12] A. M. B. Braga and G. Herrmann, "Floquet waves in anisotropic periodically layered composites," *J. Acoust. Soc. Amer.*, vol. 91, no. 3, pp. 1211–1227, 1992.
[13] P. I. Galich, N. X. Fang, M. C. Boyce, and S. Rudykh, "Elastic wave propagation in finitely deformed layered materials," *J. Mech. Phys. Solids*, vol. 98, pp. 390–410, Jan. 2017.
[14] S. I. Rokhlin and L. Wang, "Stable recursive algorithm for elastic wave propagation in layered anisotropic media: Stiffness matrix method," *J. Acoust. Soc. Amer.*, vol. 112, no. 3, pp. 822–834, 2002.
[15] M. Hamilton and D. Blackstock, *Nonlinear Acoustics*. San Diego, CA, USA: Academic, 1998.
[16] E. L. Tan, "Generalized eigenproblem of hybrid matrix for floquet wave propagation in one-dimensional phononic crystals with solids and fluids," *Ultrasonics*, vol. 50, no. 1, pp. 91–98, 2010.
[17] L. D. Landau and E. M. Lifshitz, *Theory of Elasticity*. London, U.K.: Pergamon, 1959.
[18] Y. Ishii and S. Biwa, "Transmission of ultrasonic waves at oblique incidence to composite laminates with spring-type interlayer interfaces," *J. Acoust. Soc. Amer.*, vol. 138, no. 5, pp. 2800–2810, 2015.
[19] L. Wang and S. I. Rokhlin, "Time-resolved line focus acoustic microscopy of layered anisotropic media: Application to composites," *IEEE Trans. Ultrason., Ferroelect., Freq. Control*, vol. 49, no. 9, pp. 1231–1244, Sep. 2002.
[20] F. D. Murnaghan, "Finite deformations of an elastic solid," *Amer. J. Math.*, vol. 59, no. 2, pp. 235–260, 1937.
[21] J. J. Dike and G. Johnson, "Residual stress determination using acoustoelasticity," *J. Appl. Mech., Trans. ASME*, vol. 57, no. 1, pp. 12–17, 1990.
[22] Y. Li and R. Thompson, "Influence of anisotropy on the dispersion characteristics of guided ultrasonic plate modes," *J. Acoust. Soc. Amer.*, vol. 87, no. 5, pp. 1911–1931, 1990.

Andriejus Demčenko received the B.Sc. degree in telecommunications engineering, the M.Sc. and Ph.D. degrees in measurement engineering from the Kaunas University of Technology, Kaunas, Lithuania, in 2001, 2003, and 2008, respectively, and the Ph.D. degree in mechanical engineering from the University of Twente, Enschede, The Netherlands, in 2014.

He is currently a Research Associate with the Division of Biomedical Engineering, School of Engineering, University of Glasgow, Glasgow, Scotland. His current research interests include physical linear and nonlinear ultrasonics in solid media.

Michael Mazilu was born in Bucharest, Romania, in 1969. He received the Magister degree in materials with a focus on electronic and mechanic properties and the Postgraduate Diploma degree in condensed matter and material physics from Louis Pasteur University, Strasbourg, France, and the Ph.D. degree in optoelectronics from the University of St. Andrews, St. Andrews, Scotland.

He is currently a Senior Lecturer with the School of Physics and Astronomy, University of St. Andrews. His research interests include fundamental and applied photonics and phononics.

Rab Wilson received the B.Sc. degree (Hons.) in mathematics with theoretical physics from the University of Aberdeen, Aberdeen, Scotland, in 1996, and the M.Sc. degree in advanced materials and the Ph.D. degree with a focus on ferroelectric thin films from Cranfield University, Bedfordshire, U.K., in 1998 and 2002, respectively.

He is currently a Research Associate with the University of Glasgow, Glasgow, Scotland, working on phononic crystal waveguide structures and devices.

Arno W. F. Volker received the M.Sc. degree in applied physics and the Ph.D. degree (Hons.) in geophysics from the Delft University of Technology, Delft, The Netherlands, in 1997 and 2002, respectively. In 1996, he joined TNO, Den Haag, The Netherlands, as a Student and a Staff Member in 1997. He has been working on ultrasonic measurement solutions for industrial applications for more than 20 years. He is currently a Senior Scientist with the Acoustics and Sonar Department, TNO.

Dr. Volker is a member of Society of Exploration Geophysicists and European Association of Geoscientists and Engineers.

Jonathan M. Cooper holds The Wolfson Chair in Biomedical Engineering. He is an EPSRC Research Fellow and holds a European Research Council Advanced Programme Grant. His major research interests are in ultrasonics, fluidics, and medical diagnostics.

Prof. Cooper was elected as a Fellow of the Royal Academy of Engineering (U.K.'s national academy of engineering) as well as a Fellow of the Royal Society of Edinburgh (Scotland's national academy of arts, humanities and sciences).